Inorg. Chem. **2008**, *47*, 11120−11128

Octa- and Nonanuclear Nickel(II) Polyoxometalate Clusters: Synthesis and Electrochemical and Magnetic Characterizations

Céline Pichon,[†] Pierre Mialane,*[,†] Anne Dolbecq,[†] Jérôme Marrot,[†] Eric Rivière,[‡] Bassem S. Bassil,[§] Ulrich Kortz,[§] Bineta Keita,*[,||] Louis Nadjo,[||] and Francis Sécheresse[†]

Institut Lavoisier de Versailles, UMR 8180, Université de Versailles Saint-Quentin, 45 Avenue des Etats-Unis, 78035 Versailles Cedex, France, Institut de Chimie Moléculaire et des Matériaux d'Orsay, UMR 8182, Equipe Chimie Inorganique, Université Paris-Sud 11, Bâtiment 420, 91405 Orsay, France, Laboratoire de Chimie Physique, UMR CNRS 8000, Equipe d'Electrochimie et Photoélectrochimie, Université Paris 11, Bâtiment 350, 91405 Orsay Cedex, France, and School of Engineering and Sciences, Jacobs University, P.O. Box 750561, 28725 Bremen, Germany

Received July 30, 2008

Three high-nuclearity Ni^{II}-substituted polyoxometalate compounds functionalized by exogenous ligands have been synthesized and characterized. The octanuclear complexes in $Na_{15}[Na\{(A\text{-}\alpha\text{-}SiW_9O_{34})Ni_4(CH_3COO)_3(OH)_3\}_2]\cdot 4NaCl\cdot 36H_2O$ (**1**) and $Na_{15}[Na\{(A\text{-}\alpha\text{-}SiW_9O_{34})Ni_4(CH_3COO)_3(OH)_2(N_3)\}_2]\cdot 32H_2O$ (**2**) can be described as two $\{Ni_4\}$ subunits connected via a $\{Na(CH_3COO)_6\}$ group, with the acetato ligands also ensuring in each subunit the connection between the paramagnetic centers. In **2**, two azido groups replace two of the six μ-hydroxo ligands present in **1**. The nonanuclear complex $K_7Na_7[(A\text{-}\alpha\text{-}SiW_9O_{34})_2Ni_9(OH)_6(H_2O)_6(CO_3)_3]\cdot 42H_2O$ (**3**) exhibits a double-cubane structure with two $[(A\text{-}\alpha\text{-}SiW_9O_{34})Ni_4(OH)_3]^{5-}$ subunits linked by three carbonato ligands. A ninth Ni^{II} center connected to one subunit via a carbonato ligand and a O═W group completes this asymmetric polyoxometalate. Electronic spectroscopy and electrochemical studies indicate that, while compounds **1**−**3** decompose in a pure aqueous medium, these complexes are very stable in a pH 6 acetate medium. The cyclic voltammetry pattern of each complex is constituted by a first eight-electron reduction wave followed by a second large-current intensity wave. The characteristics of the first waves of the complexes are clearly distinct from those obtained for their lacunary precursor $[A\text{-}\alpha\text{-}SiW_9O_{34}]^{10-}$, a feature that is due to the Ni centers in the complexes. Such observations of electroactive, stable, and highly nickel-rich polyoxometalates are not common. Measurements of the magnetic susceptibility revealed the occurrence of concomitant ferromagnetic and antiferromagnetic interactions in **1** and **3**. For both of these compounds, the extension of the magnetic exchange has been determined by means of a spin Hamiltonian with three and four *J* constants, respectively.

Introduction

Polyoxometalates (POMs) are discrete anionic metal−oxygen clusters and exhibit a great diversity of sizes, nuclearities, and shapes.[1] Over the past decades, these compounds have attracted extensive interest because of their applications in numerous fields such as medicine,[2] catalysis,[3] molecular magnetism,[4] electrochemistry,[5] or photochromism.[6] These properties can be tuned thanks to the high versatility of these polyanionic structures, and the design and synthesis of new 3d transition-metal-substituted polyoxotungstates remain actively explored. New POM systems are still mainly issued

* To whom correspondence should be addressed. E-mail: mialane@chimie.uvsq.fr (P.M.), bineta.keita@lcp.u-psud.fr (B.K.). Fax: (+33)-1-39254381 (P.M.), (+33)-1-69154328 (B.K.).
[†] Université de Versailles Saint-Quentin.
[‡] Université Paris-Sud 11.
[§] Jacobs University.
[||] Université Paris 11.

(1) Pope, M. T. *Heteropoly and Isopoly Oxometalates*; Springer-Verlag: Berlin, 1983.
(2) (a) Rhule, J. T.; Hill, C. L.; Judd, D. A.; Schinazi, R. F. *Chem. Rev.* **1998**, *98*, 327. (b) Hasenknopf, B. *Front. Biosci.* **2005**, *10*, 275.
(3) Polyoxometalates in Catalysis: Hill, C. L. *J. Mol. Catal. A: Chem.* **2007**, *262*, 1–242.
(4) (a) Clemente-Juan, J. M.; Coronado, E. *Coord. Chem. Rev.* **1999**, *193*−*195*, 361. (b) Mialane, P.; Dolbecq, A.; Sécheresse, F. *Chem. Commun.* **2006**, 3477.
(5) Keita, B.; Nadjo, L. Electrochemistry of Polyoxometalates. In *Encyclopedia of Electrochemistry*; Bard, A. J., Stratmann, M., Eds.; Wiley-VCH: New York, 2006; Vol. *7*.
(6) He, T.; Yao, J. *Prog. Mater. Sci.* **2006**, *51*, 810.

10.1021/ic801431f CCC: $40.75
Published on Web 10/29/2008

from the reaction of Keggin or Dawson−Wells lacunary POMs, which act as polydentate ligands toward 3d transition-metal ions. In these last years, large magnetic clusters[7] with nuclearities up to 28[8] have been reported using tri- and hexalacunary heteropolyoxometalates or the $[H_7P_8W_{48}O_{184}]^{33-}$ phosphotungstate crown ligand.

Focusing on nickel chemistry, the study of the reactivity of Ni^{II} ions with vacant polyanions in the usual bench conditions has led to the characterization of complexes with nuclearities ranging from 1 to 9. Most of these compounds exhibit a sandwich-type structure, as exemplified by the $[(As^{III}W_9O_{33})_2Ni_3(C_5H_5N)_3]^{12-}$,[9a] $[(As^{V}_2W_{15}O_{56})_2Ni_4(H_2O)_2]^{16-}$,[9b] $[(PW_9O_{34})_2Ni_3Na(H_2O)_2]^{11-}$[9c,d] and $[(PW_9O_{34})_2Ni_4(H_2O)_2]^{10-}$[9e] compounds. Besides these dimeric complexes, transition-metal-substituted monomers have also been isolated. Noticeably, one of these complexes, $[H_2PW_9O_{34}Ni_4(OH)_3(H_2O)_6]^{2-}$, contains a $\{Ni_4\}$ cluster with a cubane arrangement, a rare topology in POM chemistry. This compound has been obtained by the addition of $NiSO_4$ to $[B\text{-}\alpha\text{-}PW_9O_{34}]^{9-}$ in an acetate buffer.[10] A related species has also been synthesized directly by mixing Na_2WO_4, $Ni(CH_3COO)_2$, and Na_2HPO_4. In this case, a $\{Ni_3W\}$ group caps the trivacant precursor, leading to the trinuclear $[PW_{10}O_{39}Ni_3(H_2O)_4]^{7-}$ complex.[11] In the original banana-shaped hexanuclear $[Ni_6As_3W_{24}O_{94}(H_2O)_2]^{17-}$ complex, two trinuclear $\{B\text{-}\alpha\text{-}Ni_3AsW_9O_{40}\}$ units are connected by a $\{AsW_6O_{16}\}$ fragment.[12] More recently, Wang et al. have described the heptanuclear double-cubane-type POM $[(SiW_8O_{31})_2Ni_7(H_2O)_4(OH)_6]^{12-}$, where a Ni center is connected to two $\{Ni_3\}$ fragments.[13] Finally, the Ni^{II} POM possessing the highest nuclearity reported to date, the nonanuclear $[(PW_9O_{34})_3Ni_9(OH)_3(H_2O)_6(HPO_4)_2]^{16-}$ polyanionic cluster, was synthesized by Coronado et al. 10 years ago.[9e] It can be described as the assembly of three $\{PW_9Ni_3\}$ subunits linked by phosphato ligands. In this case, instead of using the preformed trilacunary POM, the trivacant phosphotungstate is formed in situ starting from Na_2WO_4, $Ni(CH_3COO)_2$, and Na_2HPO_4. It should be noticed that, although many of the Ni^{II} POM compounds mentioned above have been synthesized in an acetate buffer, all of these complexes are purely inorganic. More generally, among all of the 3d transition-metal-substituted polyanions synthesized in the usual bench conditions, few examples of POM systems where organic ligands bridge 3d magnetic centers have been reported.[14] We can mention here that Pope et al. reported in 1996 the first example of this family of compounds, the chromium complex $[\gamma\text{-}SiW_{10}O_{36}(OH)Cr_2(OH)(CH_3COO)_2(H_2O)_2]^{5-}$.[15] Another example of such a compound has been obtained by the reaction of the $[H_2P_2W_{12}O_{48}]^{12-}$ precursor with iron, leading to the $[H_4P_2W_{12}O_{56}Fe_9(CH_3COO)_7]^{6-}$ complex.[8] Finally, in 2007, our group has explored the reactivity of cobalt(II) silicotungstate POMs with exogeneous ligands such as acetate and carbonate, showing that functionalized cobalt POM molecular compounds can be obtained.[16]

Considering now Ni^{II}-substituted POM clusters incorporating ligands bridging the 3d centers, in addition to the phosphato-bridged nonanuclear complex mentioned above, the dinuclear $[(PW_{10}O_{37})(Ni(H_2O))_2(\mu\text{-}N_3)]^{6-}$ azido compound[17] and the heptanuclear $[(A\text{-}\alpha\text{-}SiW_9O_{34})(\beta\text{-}SiW_{10}O_{37})Ni_7(OH)_4(CO_3)_2(HCO_3)(H_2O)]^{10-}$ carbonato complex[18] have been obtained. However, the synthesis in the usual bench conditions of Ni^{II} POMs substituted by exogenous ligands largely remains to be explored. Here we report the synthesis, structure, and electrochemical and magnetic properties of two octanuclear and one nonanuclear Ni^{II} POM complexes incorporating azido, acetato, or carbonato ligands.

Experimental Section

Synthesis. All chemicals were of reagent grade and were used as received. $Na_{10}[A\text{-}\alpha\text{-}SiW_9O_{34}]\cdot 23H_2O$ was synthesized as previously described.[19]

$Na_{15}[Na\{(A\text{-}\alpha\text{-}SiW_9O_{34})Ni_4(CH_3COO)_3(OH)_3\}_2]\cdot 4NaCl\cdot 36H_2O$ (**1**): $Na_{10}[A\text{-}\alpha\text{-}SiW_9O_{34}]\cdot 23H_2O$ (1 g, 0.35 mmol) and $Ni(CH_3COO)_2\cdot 4H_2O$ (356 mg, 1.43 mmol) were dissolved in a 2 M sodium acetate solution (8 mL), and 1 mL of 0.5 M NaCl was added. The green solution was heated to 80 °C for 30 min and then cooled to room temperature. After 1 week, green hexagonal crystals suitable for X-ray diffraction were filtered, washed with a minimum amount of a 2 M NaOAc solution, and dried with ethanol and diethyl ether. Yield: 340 mg (29%). Anal. Calcd (found) for **1** ($Si_2W_{18}O_{122}Ni_8C_{12}H_{96}Na_{20}Cl_4$) (%): W, 49.92 (50.88); Ni, 7.08

(7) (a) Mal, S. S.; Dickman, M. H.; Kortz, U.; Todea, A. M.; Merca, A.; Bögge, H.; Glaser, T.; Müller, A.; Nellutla, S.; Kaur, N.; van Tol, J.; Dalal, N. S.; Keita, B.; Nadjo, L. *Chem.—Eur. J.* **2008**, *14*, 1186. (b) Pichon, C.; Dolbecq, A.; Mialane, P.; Marrot, J.; Rivière, E.; Sécheresse, F. *Dalton. Trans.* **2008**, 71. (c) Pradeep, C. P.; Long, D.-L.; Kögerler, P.; Cronin, L. *Chem. Commun.* **2007**, 4254. (d) Pichon, C.; Mialane, P.; Dolbecq, A.; Marrot, J.; Rivière, E.; Keita, B.; Nadjo, L.; Sécheresse, F. *Inorg. Chem.* **2007**, *46*, 5292. (e) Zhang, Z.; Qi, Y.; Qin, C.; Li, Y.; Wang, E.; Wang, X.; Su, Z.; Xu, L. *Inorg. Chem.* **2007**, *46*, 8162. (f) Zhao, J.-W.; Zhang, J.; Zheng, S.-T.; Yang, G.-Y. *Inorg. Chem.* **2007**, *46*, 10944. (g) Mal, S. S.; Kortz, U. *Angew. Chem., Int. Ed.* **2005**, *44*, 3777. (h) Godin, B.; Vaissermann, J.; Herson, P.; Ruhlmann, L.; Verdaguer, M.; Gouzerh, P. *Chem. Commun.* **2005**, 5624. (i) Mialane, P.; Dolbecq, A.; Marrot, J.; Rivière, E.; Sécheresse, F. *Angew. Chem., Int. Ed.* **2003**, *42*, 3523.

(8) Godin, B.; Chen, Y.-G.; Vaissermann, J.; Ruhlmann, L.; Verdaguer, M.; Gouzerh, P. *Angew. Chem., Int. Ed.* **2005**, *44*, 3072.

(9) (a) Liu, X.-M.; Wang, C.-R.; Liu, B.; Xue, G.-L.; Hu, H.-M.; Wang, J.-W.; Fu, F. *Chin. J. Chem.* **2005**, *23*, 1413. (b) Bi, L.-H.; Wang, E. B.; Peng, J.; Huang, R.-D.; Xu, L.; Hu, C.-W. *Inorg. Chem.* **2000**, *39*, 671. (c) Kortz, U.; Mbomekalle, I. M.; Keita, B.; Nadjo, L.; Berthet, P. *Inorg. Chem.* **2002**, *41*, 6412. (d) Mbomekalle, I. M.; Keita, B.; Nadjo, L.; Berthet, P. *Inorg. Chem. Commun.* **2003**, *6*, 435. (e) Clemente-Juan, J. M.; Coronado, E.; Galán-Mascarós, J. R.; Gómez-Garcia, C. J. *Inorg. Chem.* **1999**, *38*, 55.

(10) Kortz, U.; Tézé, A.; Hervé, G. *Inorg. Chem.* **1999**, *38*, 2038.

(11) Gómez-García, C. J.; Coronado, E.; Ouahab, L. *Angew. Chem., Int. Ed.* **1992**, *31*, 649.

(12) Mbomekalle, I. M.; Keita, B.; Nierlich, M.; Kortz, U.; Berthet, P.; Nadjo, L. *Inorg. Chem.* **2003**, *42*, 5143.

(13) Zhang, Z.; Wang, E.; Qi, Y.; Li, Y.; Mao, B.; Su, Z. *Cryst. Growth Des.* **2007**, *7*, 1305.

(14) (a) Botar, B.; Kögerler, P.; Hill, C. L. *Inorg. Chem.* **2007**, *46*, 5398. (b) Pradeep, C. P.; Long, D. L.; Newton, G. N.; Song, Y.-F.; Cronin, L. *Angew. Chem., Int. Ed.* **2008**, *47*, 4388. (c) Fang, X.; Kögerler, P. *Chem. Commun.* **2008**, 3396.

(15) Wassermann, K.; Lunk, H.-J.; Palm, R.; Fuchs, J.; Steinfeldt, N.; Stösser, R.; Pope, M. T. *Inorg. Chem.* **1996**, *35*, 3273.

(16) Lisnard, L.; Mialane, P.; Dolbecq, A.; Marrot, J.; Clemente-Juan, J. M.; Coronado, E.; Keita, B.; de Oliveira, P.; Nadjo, L.; Sécheresse, F. *Chem.—Eur. J.* **2007**, *13*, 3525.

(17) Mialane, P.; Dolbecq, A.; Rivière, E.; Marrot, J.; Sécheresse, F. *Angew. Chem., Int. Ed.* **2004**, *43*, 2274.

(18) Zhang, Z.; Li, Y.; Wang, E.; Wang, X.; Qin, C.; An, H. *Inorg. Chem.* **2006**, *45*, 4313.

(19) Tézé, A.; Hervé, G. *Inorg. Synth.* **1990**, *27*, 85.

(6.80); Na, 6.93 (6.91); H, 1.46 (1.51); C, 2.17 (2.12). IR (cm^{-1}, KBr disk): 1610(w), 1564(m), 1428(m), 1348(w), 990(s), 937(s), 894(s), 878(s), 858(s), 815(ms), 777(m), 706(m), 673(m), 635(sh), 521(s). UV/vis ($c = 2.5 \times 10^{-3}$ M; λ, nm (ϵ, L mol^{-1} cm^{-1})): 398 (125), 694 (45), 765 (40). The number of water molecules has been confirmed by thermogravimetric analysis (TGA; Figure SI1a in the Supporting Information).

$Na_{15}[Na\{(A\text{-}\alpha\text{-}SiW_9O_{34})Ni_4(CH_3COO)_3(OH)_2(N_3)\}_2]\cdot 32H_2O$ (**2**): $Na_{10}[A\text{-}\alpha\text{-}SiW_9O_{34}]\cdot 23H_2O$ (0.5 g, 0.17 mmol) and $Ni(CH_3COO)_2\cdot 4H_2O$ (177 mg, 0.72 mmol) were dissolved in 3 mL of a 2 M sodium acetate solution. Then, NaN_3 (70 mg, 1.07 mmol) dissolved in 1 mL of 2 M NaOAc was added. After heating to 80 °C for 30 min, the solution was cooled to room temperature and placed in a closed crystallizing dish. After 1 week, green hexagonal crystals were collected by filtration through a glass frit, washed with a minimum amount of 2 M NaOAc, and dried with ethanol and ether. Yield: 350 mg (63%). Anal. Calcd (found) for **2** ($Si_2W_{18}O_{116}Ni_8N_6C_{12}H_{86}Na_{16}$) (%): W, 51.92 (47.42); Ni, 7.37 (7.16); N, 1.32 (1.69); Na, 5.77 (6.72); H, 1.36 (1.35); C, 2.26 (2.38). IR (cm^{-1}, KBr disk): 2099(s), 1594(w), 1559(m), 1436(m), 1282(w), 975(s), 933(s), 885(s), 810(s), 777(s), 705(s), 684(sh), 525(s). UV/vis ($c = 2.5 \times 10^{-3}$ M); λ, nm (ϵ, L mol^{-1} cm^{-1})): 398 (130), 696 (50), 775(45). The number of water molecules has been confirmed by TGA (Figure SI1b in the Supporting Information).

$K_7Na_7[(A\text{-}\alpha\text{-}SiW_9O_{34})_2Ni_9(OH)_6(H_2O)_6(CO_3)_3]\cdot 42H_2O$ (**3**): $Na_{10}[A\text{-}\alpha\text{-}SiW_9O_{34}]\cdot 23H_2O$ (1 g, 0.35 mmol) and $Ni(SO_4)\cdot 7H_2O$ (0.40 g, 1.43 mmol) were dissolved in 16 mL of water, and a 2 M K_2CO_3 solution (715 μL, 1.43 mmol) was added. The solution was stirred for 1 h at room temperature. After 1 day, green parallelepipedic crystals suitable for X-ray diffraction were collected by filtration, washed with a 2 M KCl solution, and dried with ethanol and diethyl ether. Yield: 0.75 g, 65% based on W. Anal. Calcd (found) for **3** ($Si_2W_{18}O_{131}Ni_9C_3H_{102}K_7Na_7$) (%): W, 50.42 (49.44); Ni, 8.05 (8.04); K, 4.17 (4.50); Na, 2.45 (2.57); H, 1.57 (1.35); C, 0.55 (0.65). IR (cm^{-1}, KBr disk): 1634(m), 1507(m), 1494(m), 1423(m), 1381(w), 982(s), 936(s), 891(s), 860(sh), 814(s), 768(sh), 684(m), 523(s). UV/vis ($c = 5 \times 10^{-3}$ M; λ, nm (ϵ, L mol^{-1} cm^{-1})): 393 (160), 696 (50), 767(40). The number of water molecules has been confirmed by TGA (Figure SI1c in the Supporting Information).

IR spectra were recorded on an IRFT Magna 550 Nicolet spectrophotometer using the technique of pressed KBr pellets.

Electronic absorption spectra were recorded on a Perkin-Elmer lambda 19 spectrometer.

TGA. Thermogravimetry was carried out under a nitrogen/oxygen flow (60 mL min^{-1}) with a Perkin-Elmer electrobalance TGA-7 at a heating rate of 5 °C min^{-1} up to 800 °C.

Electrochemical Experiments. The solutions were deaerated thoroughly for at least 30 min with pure argon and kept under a positive pressure of this gas during the experiments. The source, mounting, and polishing of the glassy carbon (GC; Tokai, Japan) electrodes have been described.[20] The GC samples had a diameter of 3 mm. The electrochemical setup was an EG&G 273 A driven by a PC with the M270 software. Potentials are quoted against a saturated calomel electrode (SCE). The counter electrode was a platinum gauze of large surface area. All experiments were performed at room temperature. The measurements were performed in 0.4 M $CH_3COONa + CH_3COOH$ (pH 6), and the POM concentration was 2×10^{-4} M. All cyclic voltammograms were recorded at a scan rate of 10 mV s^{-1}, unless otherwise stated.

Stability Studies. Before a study of the redox properties of the reported POMs, it was necessary to determine their stability domains over the pH scale being used. In fact, it is known that polyanions may undergo chemical transformations or completely decompose depending on the pH of the solution in which they are dissolved. For the stability tests, UV/vis spectra of POM-containing solutions recorded as a function of time were compared. All solutions were 2×10^{-5} or 2×10^{-3} M in polyanion and were placed in quartz cuvettes with an optical path length of 1 or 0.2 cm. Spectra were recorded with a Lambda 19 Perkin-Elmer spectrophotometer. The lower concentration value was appropriate to monitor the absorbance of the polytungstate framework in the UV wavelength domain. Actually, spectra recorded at 2×10^{-3} M concentration show the following characteristics between 900 and 350 nm: (i) in this domain, three peaks are observed roughly at 400, 700, and 770 nm; (ii) specifically, at pH 6, the best defined peak is located at $\lambda = 689$ nm for **1**, 678 nm for **2**, and 686 nm for **3**; (iii) the spectra remain identical in both intensity and wavelength location over a period of several hours. Altogether these spectra indicate the full stability of the three POMs in the pH 6 medium (0.4 M $CH_3COONa + CH_3COOH$). The same observations are valid for pH 7 (acetate). In contrast, for media more acidic than pH 6 and whatever their composition (acetate or sulfate), the complexes are not very stable and the faster decomposition, the lower the pH. These conclusions were confirmed by cyclic voltammetry (CV). In contrast with the perfect reproducibility observed at pH 6 for voltammograms run on purpose from time to time over a period of several hours, the complex transformation of **3**, for example, at pH 5, leads to a series of voltammograms (Figure SI2 in the Supporting Information).

X-ray Diffraction. For all of the reported compounds, intensity data collections were carried out with a Bruker Nonius X8 APEX 2 diffractometer equipped with a CCD detector using monochromatized Mo Kα radiation ($\lambda = 0.71073$ Å). Complexes **2** and **3** were found to be air-sensitive. For **1** and **3**, the data were recorded at room temperature, while for complex **2**, a single crystal was mounted on a fiber glass in Paratone-N oil and intensity data collections were performed at 100 K. For **3**, a single crystal was mounted in a capilary tube. The absorption correction was based on multiple and symmetry-equivalent reflections in the data set using the *SADABS* program[21] based on the method of Blessing.[22] The structure was solved by direct methods and refined by full-matrix least squares using the *SHELX-TL* package.[23] In all of the structures, there is a discrepancy between the formulas determined by elemental analysis and the formulas deduced from the crystallographic atom list because of the difficulty in locating all of the disordered water molecules and some alkali counterions, a common feature among the structures of polyoxotungstates. It was found that complex **1** cocrystallizes with NaCl. Such cocrystallization of POMs with XCl salts (X = K, Cs) was previously observed.[7a,24] All of the atoms were refined anisotropically except for some disordered alkali counterions and free water molecules. In complex **2**, disordered

(20) Keita, B.; Nadjo, L. *J. Electroanal. Chem.* **1988**, *243*, 87.

(21) Sheldrick, G. M. *SADABS, program for scaling and correction of area detector data*; University of Göttingen: Göttingen, Germany, 1997.

(22) Blessing, R. *Acta Crystallogr.* **1995**, *A51*, 33.

(23) Sheldrick, G. M. *SHELX-TL version 5.03, Software Package for the Crystal Structure Determination*; Siemens Analytical X-ray Instrument Division: Madison, WI, 1994.

(24) (a) Zhang, C.; Howell, R. C.; Luo, Q. H.; Fieselmann, H. L.; Todaro, L. J.; Francesconi, L. C. *Inorg. Chem.* **2005**, *44*, 3569. (b) Hussain, F.; Bassil, B. S.; Kortz, U.; Kholdeeva, O. A.; Timofeeva, M. N.; de Oliveira, P.; Keita, B.; Nadjo, L. *Chem.—Eur. J.* **2007**, *13*, 4733.

Table 1. Crystallographic Data for **1**−**3**

	1	**2**	**3**
empirical formula	$Si_2W_{18}O_{122}Ni_8C_{12}H_{96}Na_{20}Cl_4Cl_4$	$Si_2W_{18}O_{116}Ni_8N_6C_{12}H_{86}Na_{16}$	$Si_2W_{18}O_{131}Ni_9C_3H_{102}K_7Na_7$
fw (g mol^{-1})	6629.28	6373.48	6402.01
temp (K)	293(2)	100(2)	293(2)
cryst syst	trigonal	trigonal	triclinic
space group	$P\bar{3}1c$ (No. 163)	$R\bar{3}$ (No. 148)	$P\bar{1}$ (No. 2)
a (Å)	11.927 20(10)	11.9660(7)	13.6466(5)
b (Å)	11.927 20(10)	11.9660(7)	22.9583(8)
c (Å)	48.4712(11)	72.753(7)	23.2340(8)
α (deg)	90	90	63.423(2)
β (deg)	90	90	73.4760(10)
γ (deg)	120	120	89.820(2)
V (Å^3)	5971.61(15)	9021.5(11)	6175.5 (4)
Z	4	3	2
d_{calc} (g cm^{-3})	3.767	3.526	3.469
cryst size (mm)	0.14 × 0.12 × 0.02	0.10 × 0.08 × 0.02	0.15 × 0.08 × 0. 04
no. of reflns (collected/unique)	70 171/5845 (R_{int} = 0.0488)	113 265/5901 (R_{int} = 0.0739)	123 932/35 749 (R_{int} = 0.0721)
GOF	1.095	1.263	1.046
R [$I > 2\sigma(I)$]	R1 (F_o)^a = 0.0773	R1 (F_o)^a = 0.0271	R1 (F_o)^a = 0.0570
	wR2 (F_o^2)^b = 0.2133	wR2 (F_o^2)^b = 0.0855	wR2 (F_o^2)^b = 0.1540
R (all data)	R1 (F_o)^a = 0.0858	R1 (F_o)^a = 0.0337	R1 (F_o)^a = 0.100
	wR2 (F_o^2)^b = 0.2342	wR2 (F_o^2)^b = 0.1012	wR2 (F_o^2)^b = 0.1938

^{a} $R1 = [\sum(|F_o| - |F_c|)]/\sum|F_c|$. ^{b} $wR2 = \{[\sum w(F_o^2 - F_c^2)^2]/\sum w(F_o^2)^2\}^{1/2}$.

azido and hydroxo ligands have been refined with site occupation factors of 0.333 and 0.666, respectively (see below). Crystallographic data are given in Table 1.

Magnetic Measurements. Magnetic susceptibility measurements were carried out with a Quantum Design SQUID magnetometer with an applied field of 1000 Oe using powder samples pressed into pellets to avoid preferential orientation of the crystallites. The independence of the susceptibility value with regard to the applied field was checked at room temperature. The susceptibility data were corrected from the diamagnetic contributions as deduced by using Pascal's constant tables. All of the magnetic data have been simulated using *MAGPACK*.[25]

Results and Discussion

Synthesis and Spectroscopic Characterization. Complexes **1** and **2** were synthesized in a 2 M sodium acetate solution acidified with 1 M HCl (pH 7) by the reaction at 80 °C of [A-α-SiW_9O_{34}]$^{10-}$ and nickel acetate (4 equiv) in the absence of NaN_3 or with NaN_3, respectively. As was observed in the case of the {Cu_6}, {Cu_{20}}, and {Co_4} azido compounds previously reported,[7d,16] even in the presence of a large excess of sodium azide, it has not been possible to substitute all of the hydroxo ligands bridging the 3d centers by azido groups (see below). These two compounds can also be obtained in pure water (pH ≈6.2), with the nickel salt affording the acetato ligands. In the case of compound **3**, an excess of potassium carbonate (4 equiv) was added to a mixture of [A-α-SiW_9O_{34}]$^{10-}$ and nickel sulfate in water (pH 8) at room temperature. In each case, single crystals were obtained from the reacting media after a few days. The IR spectra of compounds **1** and **2** are identical in the 1000−400 cm^{-1} range, exhibiting the characteristic bands of the [A-α-SiW_9O_{34}]$^{10-}$ POM. The ν_{asCOO} antisymmetric stretching vibrations are located at 1564 cm^{-1} for **1** and 1594 and 1559 cm^{-1} for **2**, and only one symmetric stretching vibration appears for both compounds (ν_{sCOO} = 1428 cm^{-1} for **1** and 1436 cm^{-1} for **2**).[26] This indicates that all of the carboxylato ligands are equivalent in **1**, while two crystallographically independent acetate ligands are present in complex **2**. Compared to the spectrum of **1**, two additional bands are observed in the IR spectrum of complex **2**. The intense band located at 2098 cm^{-1} is associated with the asymmetric stretching mode of the azide group. Its value (i.e., >2050 cm^{-1}) suggests that it acts as a μ-1,1 bridging ligand.[27] The second band, situated at 1280 cm^{-1}, is attributed to the symmetric stretching mode of the N_3^- group and confirms the presence of an asymmetric azido ligand. Concerning compound **3**, its IR spectra also revealed that the [A-α-SiW_9O_{34}]$^{10-}$ ligand is maintained during the synthetic process. The bands located at 1381, 1423, and 1494 cm^{-1} are characteristic of two bidentate bridging carbonato ligands.[28] The visible electronic spectra in water of complexes **1**−**3** are highly reminiscent to that of compound [$SiW_{11}O_{39}Ni(H_2O)$]$^{6-}$, with three bands situated at ca. 400, 700, and 770 nm, respectively, which are attributed to d−d transitions of the octahedral Ni^{II} centers. These spectra slightly evolve with time, showing that these complexes are not stable in this medium. Nevertheless, it has been found that the three complexes reported therein are stabilized over hours in a pH 6 acetate medium, allowing electrochemical investigations (see below).

Structures of Complexes 1 and 2. The structure of compound **1** is analogous to that found in the Co^{II} complex K_5Na_3[(A-α-SiW_9O_{34})$Co_4(OH)_3(CH_3COO)_3$]·$18H_2O$ previously reported by our group.[16] In **1**, a {Ni_4O_3}-deficient cubane-type cluster with three crystallographically equivalent Ni^{II} ions (labeled Ni1) is connected to the trivacant silico-

(25) Borras-Almenar, J. J.; Clemente-Juan, J. M.; Coronado, E.; Tsukerblat, B. S. *J. Comput. Chem.* **2001**, *22*, 985.

(26) Nakamoto K. *Infrared and Raman Spectra of Inorganic and Coordination Compounds. Part B: Applications in Coordination, Organometallic and Bioinorganic Chemistry*, 5th ed.; John Wiley & Sons: New York, 1997; Vol. *59*.

(27) Tandon, S. S.; Thompson, L. K.; Manuel, M. E.; Bridson, J. N. *Inorg. Chem.* **1994**, *33*, 5555.

(28) Gatehouse, B. M.; Livingstone, S. E.; Nyholm, R. S. *J. Chem. Soc.* **1958**, 3137.

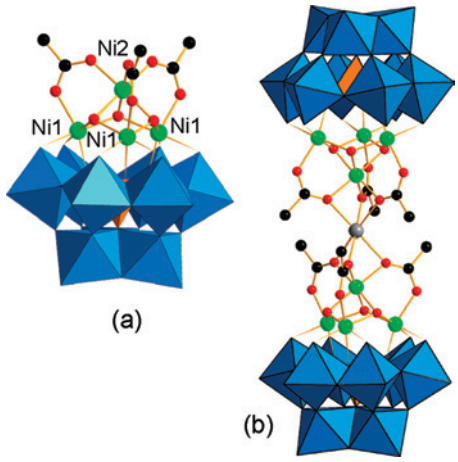

Figure 1. (a) Polyhedral and ball-and-stick representation of the $[SiW_9O_{34}Ni_4(OH)_3(CH_3COO)_3]^{8-}$ subunit in **1**. (b) Polyhedral and ball-and-stick representation of the dimeric complex **1**. Color code: blue octahedra, $\{WO_6\}$; orange tetrahedra, $\{SiO_4\}$; green spheres, Ni; gray sphere, Na; red spheres, O; black spheres, C.

tungstate ligand. The Ni1 atoms are inserted in the vacancies of the polyanion and capped by an additional Ni^{II} center (labeled Ni2) via three acetato bridges and three hydroxo ligands, with a C_3 axis passing through Ni2 and the Si atom (Figure 1a). All of the Ni atoms are in an octahedral environment. Ni1 is tricoordinated to the trivacant polyanion [$d_{Ni1-O(W)} = 2.048(5)-2.054(7)$ Å and $d_{Ni1-O(Si)} = 2.212(6)$ Å] and connected to two μ_3-OH ligands [$d_{Ni1-O(H)} = 2.002(7)-2.038(7)$ Å; Ni1−O(H)−Ni1 = 131.3(3)°]. The nature of the hydroxo bridges has been confirmed by bond valence sum calculations (BVS = 1.09).[29] The coordination sphere of Ni1 is completed by an O atom of an acetato ligand [$d_{Ni1-O(OCCH3)} = 2.076(7)$ Å]. Ni2 is coordinated to the three hydroxo and acetato groups [$d_{Ni2-O(H)} = 2.049(5)$ Å; $d_{Ni2-O(OCCH3)} = 2.041(7)$ Å; Ni1−O(H)−Ni2 = 91.590(2)°], affording the $[SiW_9O_{34}Ni_4(OH)_3(CH_3COO)_3]^{8-}$ subunit. Finally, two subunits are linked via a Na cation hexacoordinated to six O atoms [$d_{Na-O} = 2.321(7)$ Å] of the six acetato groups constituting the two tetranuclear fragments, leading to a dimeric octanuclear compound (Figure 1b). Such a linkage of Ni^{II} centers via a $\{Na(RCOO)_6\}$ group (R = CH_3, H) has recently been observed for complexes bearing organic ligands.[30]

In a comparison of complex **1** to the $[H_2PW_9O_{34}Ni_4(OH)_3(H_2O)_6]^{2-}$ compound previously characterized by Kortz et al.[10] and which can also be described as a trivacant POM ligand capped by a tetranuclear $\{Ni_4\}$ fragment, three main differences must be underlined. First, the silicotungstate compound **1** is an A-type POM, while Kortz's phosphatotungstate complex is a B-type POM. This implies that in this last complex the $\{Ni_4\}$ group forms an almost regular tetrahedron, while in **1**, the $\{Ni_4\}$ group is highly distorted (Figure SI3 in the Supporting Information). It follows that in a comparison of the topologies of the $\{Ni_3\}$ fragments constituted by the Ni centers directly connected to the POM ligands the Ni−O−Ni angles are significantly larger in **1** [129.9(7)°] than in the phosphatotungstate complex [90.6(5)° ≤ Ni−O−Ni ≤ 103.5(6)°]. This structural difference must have a dramatic influence on the respective magnetic behavior of these two complexes (see below). Second, while both **1** and the $[H_2PW_9O_{34}Ni_4(OH)_3(H_2O)_6]^{2-}$ complex are synthesized in an acetate buffer, no organic group connects the Ni^{II} center in this last compound, and despite several attempts, we have not been able to obtain the carboxylato derivative of the nickel(II) phosphatotungstate compound. This can be explained by simple topological considerations. In the complex $[H_2PW_9O_{34}Ni_4(OH)_3(H_2O)_6]^{2-}$, because of the B-type nature of the POM ligand, the shortest distances between the water molecules connected to the Ni^{II} cations are too long (2.77 Å ≤ $d_{OH2-OH2}$ ≤ 3.12 Å) to allow their replacement by chelating carboxylato groups. In contrast, the A-type nature of the POM ligand in compound **1** allows the connection of chelating acetate ligands, with the distances between the apical O atoms of the Ni^{II} centers being then of 2.24 Å. Third, the $[H_2PW_9O_{34}Ni_4(OH)_3(H_2O)_6]^{2-}$ compound can be described as an isolated tetranuclear complex, while in compound **1**, the connection between two subunits via a $\{Na(CH_3COO)_6\}$ group implies that the Ni2−Ni2 distance is relatively short (5.83 Å). Again, this structural difference can have consequences on the magnetic properties of complex **1**.

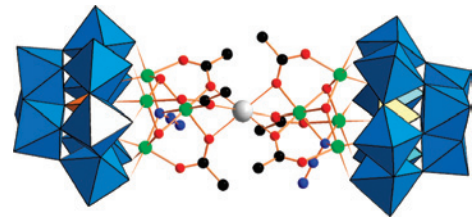

Figure 2. Polyhedral and ball-and-stick representation of compound **2**. Color code: blue octahedra, $\{WO_6\}$; orange tetrahedra, $\{SiO_4\}$; green spheres, Ni; gray sphere, Na; red spheres, O; blue spheres, N; black sphere, C.

Compound **2** crystallizes in the $R\bar{3}$ space group and is represented in Figure 2. This compound has the same arrangement as **1**, with the only difference being that in **2** the hydroxo ligands bridging the Ni1 atoms are partially substituted by μ-1,1 azido ligands. The presence of the C_3 axis causes a disorder between the azido and hydroxo bridging groups. The structure has been refined with occupancy factors of $^2/_3$ for μ_3-OH and $^1/_3$ for μ_3-N_3, leading to the formulation $[Na\{(A\text{-}\alpha\text{-}SiW_9O_{34})Ni_4(CH_3COO)_3(OH)_2(N_3)\}_2]^{15-}$.

Structure of Complex $K_7Na_7[(A\text{-}\alpha\text{-}SiW_9O_{34})_2Ni_9(OH)_6(H_2O)_6(CO_3)_3]\cdot 37H_2O$ (3). The nonanuclear compound **3** has an asymmetric dimeric structure composed of two $[\alpha\text{-}SiW_9O_{34}Ni_4(OH)_3]^{5-}$ subunits linked by three carbonato ligands, with an additionnal Ni atom connected to one subunit via one of the CO_3^{2-} bridging ligands and a W=O group (Figure 3). As in compounds **1** and **2**, each subunit consists of a tetranuclear cluster constituted of a $\{Ni_3(OH)_3\}$ fragment [$d_{Ni-O(H)} = 1.997(10)-2.044(9)$ Å] embedded in the lacuna of a $\{A\text{-}\alpha\text{-}SiW_9O_{34}\}$ polyanion and capped by a Ni center,

(29) Brese, N. E.; O'Keefe, O. *Acta Crystallogr.* **1991**, *B47*, 192.
(30) (a) Biswas, B.; Khanra, S.; Weyhermüller, T.; Chaudhuri, P. *Chem. Commun.* **2007**, 1059. (b) Adams, H.; Fenton, D. E.; McHugh, P. E. *Inorg. Chem. Commun.* **2004**, *7*, 147. (c) Adams, H.; Fenton, D. E.; McHugh, P. E. *Inorg. Chem. Commun.* **2004**, *7*, 880.

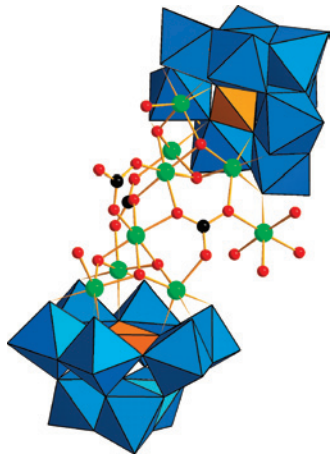

Figure 3. Polyhedral and ball-and-stick representation of compound **3**. Color code: blue octahedra, $\{WO_6\}$; orange tetrahedra, $\{SiO_4\}$; green spheres, Ni; red spheres, O; black spheres, C.

with the μ_3-OH ligands linking the Ni atoms of the $\{Ni_3\}$ fragment also ensuring the connection with the capping Ni atom [$d_{Ni-O(H)} = 2.053(10)-2.088(9)$ Å]. The three carbonato ligands are crystallographically inequivalent with one μ_4-η^1:η^1:η^2 CO_3^{2-} group, one μ_2-η^1:η^1 CO_3^{2-} ligand, and one μ_5-η^1:η^2:η^2 carbonato group [$d_{Ni1-O(CO2)} = 2.037(9)-2.120(9)$ Å and $d_{Ni2-O(CO2)} = 2.039(10)-2.084(9)$ Å]. The structure of compound **3** can then be compared to the octanuclear Co^{II} complex $[(A\text{-}\alpha\text{-}SiW_9O_{34})_2Co_8(OH)_6(H_2O)_2(CO_3)_3]^{16-}$ previously reported, where two $\{Co_4\}$ units are connected by three carbonato ligands.[16] The ninth Ni^{II} ion is grafted to one subunit via the μ_5-η^1:η^2:η^2 CO_3^{2-} ligand [$d_{Ni-O(CO2)} = 2.093(10)$ Å] and one terminal O atom of the POM [$d_{Ni-O(W)} = 2.017(9)$ Å]. The coordination sphere of this additional Ni center is completed by four aquo ligands [BVS = 0.33−0.37; $d_{Ni-O(H2)} = 2.025(12)-2.061(11)$ Å].

Complex **3** can also be compared to the heptanuclear complex $[(A\text{-}\alpha\text{-}SiW_9O_{34})(\beta\text{-}SiW_{10}O_{37})Ni_7(OH)_4(CO_3)_2(HCO_3)(H_2O)]^{10-}$,[18] which represents to date the only other example of a carbonato Ni^{II} POM. For this latter compound, the magnetic cluster is embedded between divacant and trivacant POM ligands, while in **3**, two trivacant silicotungstate POMs encapsulate the 3d fragment, justifying the higher nuclearity of complex **3** compared to the compound $[(A\text{-}\alpha\text{-}SiW_9O_{34})(\beta\text{-}SiW_{10}O_{37})Ni_7(OH)_4(CO_3)_2(HCO_3)(H_2O)]^{10-}$.

Magnetic Properties. Because of the structural complexity of complexes **1** and **3**, an interpretation of their magnetic data necessitates four and five independent parameters, respectively, even if a simplified model is taken into account (see below). The case of compound **2** is even more complicated because of the presence of a disordered azido ligand, and the magnetic properties of this compound have not been investigated.

For complex **1**, the $\chi_M T$ product continuously decreases from 300 K ($\chi_M T = 8.65$ cm^3 mol^{-1} K, with the $\chi_M T$ value calculated for eight noninteracting Ni^{II} centers being 8.82 cm^3 mol^{-1} K, assuming $g = 2.1$) to 2 K ($\chi_M T = 2.72$ cm^3 mol^{-1} K), indicating that antiferromagnetic exchange interactions are predominant in this compound. A first approach to quantify the magnetic interactions in **1** has been performed

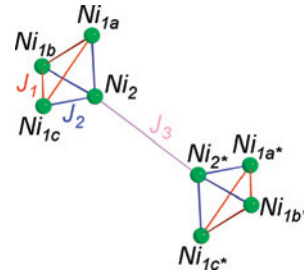

Figure 4. Coupling scheme adopted for complex **1**.

considering that the $[SiW_9O_{34}Ni_4(OH)_3(CH_3COO)_3]^{8-}$ subunits are magnetically isolated. The corresponding isotropic Hamiltonian (1) can then be written as

$$\hat{H} = -J_1(\hat{S}_{Ni1a}\hat{S}_{Ni1b} + \hat{S}_{Ni1b}\hat{S}_{Ni1c} + \hat{S}_{Ni1c}\hat{S}_{Ni1a}) - J_2(\hat{S}_{Ni1a}\hat{S}_{Ni2} + \hat{S}_{Ni1b}\hat{S}_{Ni2} + \hat{S}_{Ni1c}\hat{S}_{Ni2}) \quad (1)$$

with $S_{Ni1a} = S_{Ni1b} = S_{Ni1c} = S_{Ni2} = 1$ and J_1 and J_2 relating the Ni1···Ni1 and Ni1···Ni2 interactions, respectively (Figure 4). A best fit to the experimental $\chi_M T$ data in the 300−5 K temperature range afforded $J_1 = -13.9$ cm^{-1}, $J_2 = +4.4$ cm^{-1}, and $g = 2.16$. While the obtained fit is acceptable ($R = 2.5 \times 10^{-4}$),[31] there are noticeable discrepancies in the whole range of temperature (Figure SI4 in the Supporting Information). Bearing in mind that in **1** two $\{Ni_4\}$ fragments are connected via a $\{Na(CH_3COO)_6\}$ group, we have then treated the data considering the whole $\{Ni_8\}$ cluster. This implies taking into consideration an additional J_3 exchange parameter reflecting the Ni2···Ni2 spin interaction (Figure 4). The following Hamiltonian (2) has then been considered:

$$\hat{H} = -J_1(\hat{S}_{Ni1a}\hat{S}_{Ni1b} + \hat{S}_{Ni1b}\hat{S}_{Ni1c} + \hat{S}_{Ni1c}\hat{S}_{Ni1a} + \hat{S}_{Ni1a*}\hat{S}_{Ni1b*} + \hat{S}_{Ni1b*}\hat{S}_{Ni1c*} + \hat{S}_{Ni1c*}\hat{S}_{Ni1a*}) - J_2(\hat{S}_{Ni1a}\hat{S}_{Ni2} + \hat{S}_{Ni1b}\hat{S}_{Ni2} + \hat{S}_{Ni1c}\hat{S}_{Ni2} + \hat{S}_{Ni1a*}\hat{S}_{Ni2*} + \hat{S}_{Ni1b*}\hat{S}_{Ni2*} + \hat{S}_{Ni1c*}\hat{S}_{Ni2*}) - J_3(\hat{S}_{Ni2}\hat{S}_{Ni2*}) \quad (2)$$

The best-fit parameters obtained are $J_1 = -18.9$ cm^{-1}, $J_2 = +6.0$ cm^{-1}, $J_3 = +1.1$ cm^{-1}, and $g = 2.21$, giving an excellent fit ($R = 2.8 \times 10^{-5}$)[31] of the data in the 300−5 K range (Figure 5). It should be noticed that the Hamiltonian (2) does not take into account the single-ion anisotropy (ZFS) of the Ni^{II} centers, explaining that a deviation of the experimental values from the calculated curve is observed for $T < 10$ K (Figure SI5 in the Supporting Information). A fit of the data considering the Hamiltonian (3) defined as

$$\hat{H}(3) = \hat{H}(2) + D_{Nix}[\hat{S}_z^2 - S(S+1)] \quad (3)$$

where D_{Nix} stands for the local axial magnetic anisotropy of the paramagnetic centers, has also been performed. The best-fit parameters obtained with this computing model are $J_1 = -17.9$ cm^{-1}, $J_2 = +5.2$ cm^{-1}, $J_3 = +1.1$ cm^{-1}, $|D_{Ni}| = 3.7$ cm^{-1}, and $g = 2.21$ ($R = 9.5 \times 10^{-5}$).[31] While the $\chi_M T = f(T)$ curve calculated from these parameters allows reproduction of the experimental data in the whole 300−2 K

(31) $R = [\Sigma(\chi_M T_{calc} - \chi_M T_{obs})^2/\Sigma(\chi_M T_{obs})^2]$.

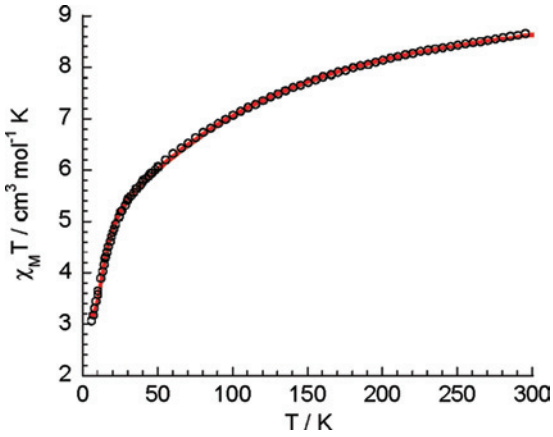

Figure 5. Thermal dependence of $\chi_M T$ for **1**. The solid line represents the best-fit parameters using Hamiltonian (2) (see the text).

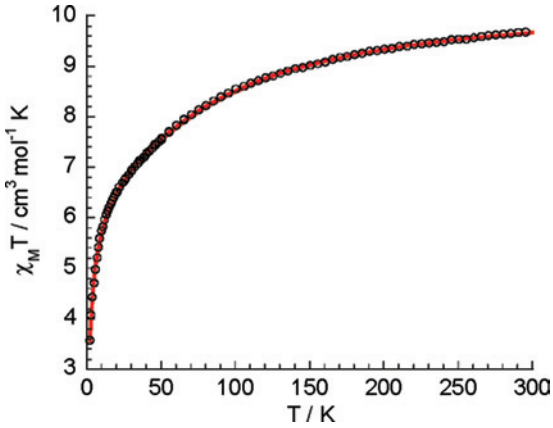

Figure 6. Thermal dependence of $\chi_M T$ for **3**. The solid line represents the best-fit parameters using Hamiltonian (4) (see the text).

temperature range, this is not the case for the $M = f(H/T)$ curves. This could be explained considering that in our model the magnetic anisotropy of the Ni1 and Ni2 centers are considered as equivalent, which represents an oversimplification. Furthermore, our model considers that the D_{Ni} tensors are collinear, which is probably not the case. Then, the determined value of D_{Ni} must be considered with care. The energy diagram derived from the parameters calculated from Hamiltonian (2) can be calculated, showing the presence of a $S = 2$ ground state with a first excited state $S = 1$ located at 4.0 cm^{-1}.

The values of the J_1 and J_2 parameters are in agreement with the expectation that the Ni^{II} e_g electrons will couple through p orbitals ferromagnetically for Ni−O−Ni angles close to 90° (Ni1−O−Ni2 = 90.4 and 91.4°; $J_2 = +6.0$ cm^{-1}) and antiferromagnetically for larger Ni−O−Ni angles (Ni1−O−Ni1 = 131.2°; $J_1 = -18.9$ cm^{-1}).[32] This explains why there is the simultaneous occurrence of ferromagnetic and antiferromagnetic interactions in **1**, while for the $[H_2PW_9O_{34}Ni_4(OH)_3(H_2O)_6]^{2-}$ POM complex[10] discussed above, which exhibits Ni−O−Ni angles in the 95.8−103.5° range, a $S = 4$ ground state is observed. It is more difficult

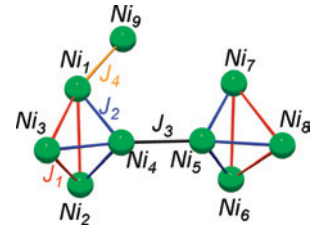

Figure 7. Coupling scheme adopted for complex **3**.

to discuss the nature of the spin interaction reflected by the J_3 parameter because, to the best of our knowledge, no quantification of the Ni···Ni interaction via a $\{Na(CH_3COO)_6\}$ bridge has been reported previously. We can just note that the weak value of J_3 determined is in agreement with the long Ni2···Ni2 distance ($d_{Ni2\cdots Ni2} = 5.83$ Å).

The $\chi_M T = f(T)$ curve related to complex **3** is represented in Figure 6. As observed for **1**, $\chi_M T$ continuously decreases from 300 K ($\chi_M T = 9.67$ cm^3 mol^{-1} K, with the $\chi_M T$ value calculated for nine noninteracting Ni^{II} centers being 9.92 cm^3 mol^{-1} K, assuming $g = 2.1$) to 2 K ($\chi_M T = 2.36$ cm^3 mol^{-1} K), revealing the overall antiferromagnetic behavior of **3**. The coupling scheme has been established considering that only the paramagnetic centers directly bridged by an O atom are magnetically interacting (Figure 7). Thus, the spin Hamiltonian can be written as

$$\hat{H} = -J_1(\hat{S}_{Ni1}\hat{S}_{Ni2} + \hat{S}_{Ni2}\hat{S}_{Ni3} + \hat{S}_{Ni3}\hat{S}_{Ni1} + \hat{S}_{Ni6}\hat{S}_{Ni7} + \hat{S}_{Ni7}\hat{S}_{Ni8} + \hat{S}_{Ni8}\hat{S}_{Ni6}) - J_2(\hat{S}_{Ni4}\hat{S}_{Ni1} + \hat{S}_{Ni4}\hat{S}_{Ni2} + \hat{S}_{Ni4}\hat{S}_{Ni3} + \hat{S}_{Ni5}\hat{S}_{Ni6} + \hat{S}_{Ni5}\hat{S}_{Ni7} + \hat{S}_{Ni5}\hat{S}_{Ni8}) - J_3(\hat{S}_{Ni4}\hat{S}_{Ni5}) - J_4(\hat{S}_{Ni1}\hat{S}_{Ni9}) \quad (4)$$

An excellent fit in the 300−2 K temperature range (Figure 6) is obtained for $J_1 = -8.3$ cm^{-1}, $J_2 = +4.9$ cm^{-1}, $J_3 = +0.8$ cm^{-1}, $J_4 = -29.4$ cm^{-1}, and $g = 2.21$ ($R = 1.1 \times 10^{-5}$).[31] As mentioned above in the case of complex **1**, the respective signs of the exchange parameters J_1 and J_2 can be justified considering the values of the Ni−O−Ni bridging angles ($\theta_{av} = 128.7°$, $J_1 = -8.3$ cm^{-1}; $\theta_{av} = 93.6°$, $J_2 = +4.9$ cm^{-1}). The J_3 parameter is found to be surprisingly low if we refer to other carbonato-bridged $\{Ni-O(CO_2)-Ni\}$ compounds previously magnetically characterized. Again, in these systems, a correlation between the exchange parameter and the Ni−O−Ni angle has been found ($\theta = 174.1°$, $J = -94.1$ cm^{-1};[33a] $\theta = 141.4°$, $J_1 = -57.7$ cm^{-1};[33b] $\theta = 105.3°$, $J_1 = -28.6$ cm^{-1}).[33c] In complex **3**, the average Ni−O(CO_2)−Ni angle is equal to 96.4°. We can then propose that such a bridging angle coincides with the situation where $|J_F| \approx |J_{AF}|$,[34] leading to an apparent uncoupling ($J = J_F + J_{AF} \approx 0$) of the spins located on the Ni4 and Ni5 centers. Finally, the lack of magnetostructural information on $\{Ni(\mu\text{-}(O(CO_2))(\mu\text{-}O(W))Ni\}$ systems precludes any considerations

(32) For example, see: (a) Clemente-Juan, J. M.; Chansou, B.; Donnadieu, B.; Tuchagues, J.-P. *Inorg. Chem.* **2000**, *39*, 5515. (b) Moragues-Cánovas, M.; Helliwell, M.; Ricard, L.; Rivière, E.; Wernsdorfer, W.; Brechin, E.; Mallah, T. *Eur. J. Inorg. Chem.* **2004**, 2219.

(33) (a) Rawle, S. C.; Harding, C. J.; Moore, P.; Alcock, N. W. *J. Chem. Soc., Chem. Commun.* **1992**, 1701. (b) Escuer, A.; Vicente, R.; Kumar, S. B.; Solans, M.; Font-Bardia, M.; Caneshi, A. *Inorg. Chem.* **1996**, *35*, 3094. (c) Escuer, A.; Vicente, R.; Kumar, S. B.; Mautner, F. A. *J. Chem. Soc., Dalton Trans.* **1998**, 3474.

(34) Kahn, O. *Molecular Magnetism*; VCH Publishers: New York, 1993.

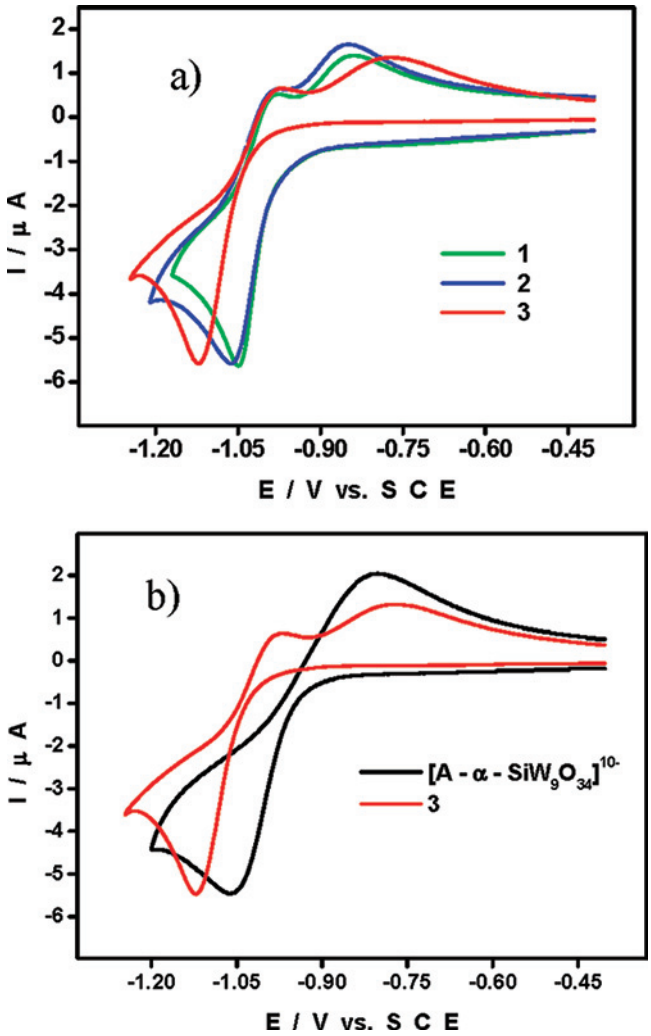

Figure 8. Cyclic voltammograms of 2×10^{-4} M solutions of **1**−**3** and $[A\text{-}\alpha\text{-}SiW_9O_{34}]^{10-}$, in a pH 6 medium (0.4 M $CH_3COONa + CH_3COOH$). The scan rate was 10 mV s^{-1}, the working electrode was GC, and the reference electrode was SCE. (a) Superposition of **1**−**3**. (b) Superposition of **3** and $[A\text{-}\alpha\text{-}SiW_9O_{34}]^{10-}$. The CV of $[A\text{-}\alpha\text{-}SiW_9O_{34}]^{10-}$ was scaled up to make its peak current match that observed with **3**.

on the determined J_4 parameter.

Electrochemistry. In the large family of multinickel-substituted POMs, few are stable in the aqueous media classically used as supporting electrolytes in electrochemical studies of POMs.[35] Fortunately, in a pH 6 acetate medium, the complexes **1**−**3** are sufficiently stable for their electrochemical study to be carried out. These electrochemical characteristics were compared to those of their lacunary precursor $[A\text{-}\alpha\text{-}SiW_9O_{34}]^{10-}$, which is also relatively stable in this medium. This precursor represents one of the possible decomposition products of the three complexes.

Figure 8a shows the CV patterns obtained in a pH 6 acetate medium for 2×10^{-4} M solutions of **1**−**3**. The three CVs have the same general shape. However, the first reduction waves of **1**−**3** peak respectively at −1.048, −1.070, and −1.118 V vs SCE, which means that, among the three compounds, **3** is the most difficult to reduce. This wave is attributed to the reduction of W centers. Figure 8b shows unambiguously that the complexes and their lacunary precursor $[A\text{-}\alpha\text{-}SiW_9O_{34}]^{10-}$ have distinct CV patterns. To highlight these differences, the CV of $[A\text{-}\alpha\text{-}SiW_9O_{34}]^{10-}$ was scaled up to make its peak current match that observed with the other complexes. The shapes of the reduction waves of the complexes and $[A\text{-}\alpha\text{-}SiW_9O_{34}]^{10-}$ are the same, but the W waves of the complexes are driven in the negative direction, in agreement with previous observations made with different Ni-substituted polyoxometalates.[36] In general, this observation is most likely related to the differences in pK_a in the reduced forms and to the overall negative charge of the POMs. Detailed parameters of the substituent cation like size, electronic configuration, and coordination geometry including possible distortions (e.g., Jahn−Teller) may also contribute to this observation.[36] Moreover, the characteristics of the reoxidation waves associated with the first reduction process of the nickel complexes and $[A\text{-}\alpha\text{-}SiW_9O_{34}]^{10-}$ are different (Figure 8b). The reoxidation pattern obtained with $[A\text{-}\alpha\text{-}SiW_9O_{34}]^{10-}$ is broad, while for the nickel complexes, this wave splits into two waves. Such an observation is not uncommon in the POM electrochemical literature when the CV patterns are compared for a complex and its lacunary precursor and can be obtained for the reduction process, the reoxidation process, or both. The explanation given above for the difference of reduction peak potential locations still holds here. In the case in which a relatively slow dissociation (on the voltammetric time scale) of the reduced form of the complex does not partially give back the lacunary precursor, this behavior was found to depend on the pH of the electrolyte, on the nature of the precursor lacunary species, and on the identity of the substituent metallic cation in the complex. It may be due to the difference in the pK_a values on the various reduced species in a multielectron process[37] and even to pK_a inversion between these species in some cases.[16,38]

It is known that the reduction of $[A\text{-}\alpha\text{-}SiW_9O_{34}]^{10-}$ is a four-electron process.[19] The number of electrons of the first reduction waves of the complexes reported here was evaluated by determining the area delimited by the relevant voltammograms and comparing the charges corresponding to each wave. This method was used to compare the complexes and $[A\text{-}\alpha\text{-}SiW_9O_{34}]^{10-}$. The charge ratio was 2 ± 0.1 in favor of the complexes, thus indicating eight electrons per molecule for the first reduction wave of the complexes. As a second method, controlled-potential coulometry was carried out at −1 V vs SCE, but the number of electrons exceeds eight because of an unidentified catalytic and/or decomposition process. Such behavior was also observed with other POMs.[39] Whatever the complex, the first wave is followed by a large-intensity second wave (not

(35) Jabbour, D.; Keita, B.; Mbomekalle, I. M.; Nadjo, L.; Kortz, U. *Eur. J. Inorg. Chem.* **2004**, 2036.

(36) Keita, B.; Girard, F.; Nadjo, L.; Contant, R.; Canny, J.; Richet, M. *J. Electroanal. Chem.* **1999**, *478*, 76.

(37) (a) Bassil, B. S.; Dickman, M. H.; Reicke, M.; Kortz, U.; Keita, B.; Nadjo, L. *Dalton Trans.* **2006**, 4253. (b) Keita, B.; Mbomekalle, I.-M.; Lu, Y.-W.; Nadjo, L.; Berthet, P.; Anderson, T. M.; Hill, C. L. *Eur. J. Inorg. Chem.* **2004**, 3462.

(38) Keita, B.; Lu, Y.-W.; Nadjo, L.; Contant, R. *Electrochem. Commun.* **2000**, *2*, 720.

(39) Hussain, F.; Kortz, U.; Keita, B.; Nadjo, L; Pope, M. T. *Inorg. Chem.* **2006**, *45*, 761.

shown), which is the combination of irreversible multielectron reduction of the complex and the electrolyte discharge. Reductive deposition phenomena are associated with this second combined wave. Such phenomena are known and have been described for a large variety of POMs.[40] In contrast, perfect reproducibility of the CV pattern was observed when the successive scans were restricted to the first wave of the complexes. The duration of the CV stability tests can last up to 10 h. To the best of our knowledge, such observations of electroactive and stable multinickel-subtituted POMs containing more than seven Ni centers are unprecedented.

Conclusion

We have reported herein the synthesis and characterization of three high-nuclearity molecular Ni^{II}-substituted POM compounds. The structure of these complexes is directed by the nature of the ligand present in the reacting media (acetate vs carbonate). To the best of our knowledge, **1** and **2** are the first examples of Ni^{II} POMs functionalized by acetate ligands, while the nonanuclear complex **3** represents, together with the $[(PW_9O_{34})_3Ni_9(OH)_3(H_2O)_6(HPO_4)_2]^{16-}$ polyanionic cluster isolated by Coronado et al. in 1999,[9e] the Ni^{II} POM with the highest nuclearity reported to date. Electronic spectroscopy and electrochemical studies indicate that compounds **1**−**3** are not stable in a pure aqueous medium. Nevertheless, the electrochemical study of the complexes in a pH 6 acetate medium offers interesting first examples of highly nickel-rich and stable POMs. The magnetic data of complexes **1** and **3** have been studied and interpreted, revealing in both compounds the occurrence of concomitant ferromagnetic and antiferromagnetic exchange interactions that have been quantified.

Acknowledgment. This work was supported by the CNRS (UMR 8000, 8180, and 8182), the Ministère de l'Education Nationale, de l'Enseignement Supérieur et de la Recherche (MENESR), and Grant ANR-06-JCJC-0146-01.

Supporting Information Available: X-ray crystallographic files, in CIF format, for **1**−**3**, TGA of these complexes (parts a−c of Figure SI1, respectively), evolution of the cyclic voltammograms of a 2×10^{-4} M solution of **3** at pH 5 as a function of time (Figure SI2), comparison of the $\{Ni_4\}$ tetranuclear fragments in **1** and in compound $Cs_2[H_2PW_9O_{34}Ni_4(OH)_3(H_2O)_6]\cdot 5H_2O$ (Figure SI3), thermal dependence of $\chi_M T$ for **1** fitted considering the Hamiltonian (1) (Figure SI4), and thermal dependence of $\chi_M T$ for **1** fitted considering the Hamiltonian (2) in the 20−2 K temperature range (Figure SI5). This material is available free of charge via the Internet at http://pubs.acs.org.

IC801431F

(40) Keita, B.; Nadjo, L. *Mater. Chem. Phys.* **1989**, *22*, 77.